

Two-dimensional nano hybridization of gold nanorods and polystyrene colloids

Dong Kee Yi,¹ Jin-Hyon Lee,² John A. Rogers,³ and Ungyu Paik^{2,a)}

¹Division of Bionanotechnology, Gachon Bionano Institute, Kyungwon University, Geonggi-do 461-701, Republic of Korea

²Division of Materials Science Engineering, Hanyang University, Seoul 133-79, Republic of Korea

³Department of Materials Science and Engineering, University of Illinois at Urbana-Champaign, Urbana, Illinois 61801, USA

(Received 23 December 2008; accepted 29 January 2009; published online 27 February 2009)

Zero-dimensional (0D) and one-dimensional (1D) nanomaterials can be coarrayed in a cocontinuous manner using convective force driven self-assembly to obtain hybrid nanomaterials. The process is demonstrated using 0D polystyrene colloids and 1D Au nanorods. The flexural properties of the spherical colloidal templates and the concentration of the nanosized building-blocks are crucial parameters that determine the dominant rod-colloid hybrid nanoarrays that are obtained. Plasmon resonance phenomena in the resulting hybrid systems are examined by ultraviolet-visible transmission/absorbance spectroscopy. The resulting coarrayed nanostructures show variable optical stop bands dependent on the angle of the incident light relative to the plane of the coarrayed film. © 2009 American Institute of Physics. [DOI: 10.1063/1.3089219]

This letter reports the fabrication of ordered hybrid structures of zero-dimensional colloids and one-dimensional nanorods formed using a confined convective array method. Certain classes of advanced materials and devices take advantage of colloidal arraying techniques^{1–5} in bottom-up nanoscale assembly methods to achieve highly functional and miniaturized structures with low cost and simple procedures. For example, two-dimensional (2D) hexagonally arrayed submicron sized polystyrene and silica colloids form regularly ordered patterns exhibiting trigonal vacancies between colloids that can be converted into metallic nanostructures.⁶ These platforms can be used, for example, as catalytic seeds to grow carbon nanotubes (CNTs) (Ref. 7) and silicon nanowires.⁸

We recently reported the formation of networks of flexible CNTs using related colloidal templating techniques.⁹ Here we explore the ability of this type of approach to create assemblies of rigid, metallic nanorods. The resulting structures are of interest partly due to their potential to achieve useful optical properties such as photonic band gap effects. An attractive feature of the method is that its facile and single-step process compared to, for example, imprinting transfer techniques.¹⁰ The strategies reported here enable tailoring of the colloidal crystal structures at the level of a monolayer to form 2D patterns.¹¹ In this mode, the materials utilization can be high: less than 20 μl (approximately 1 wt %) of starting solution can yield structures that cover a few cm^2 area within several minutes. We use this approach to form ordered, cocontinuous array patterns of Au nanorod-colloid 2D nanostructures templated onto monolayered colloid thin films. These hybrid nanocomposite materials have potential for optoelectronic and photonic devices, e.g., optical stop band modulator and biosensor, using surface plasmonic resonance effects.

Au nanorods were synthesized as described previously.¹² The resulting Au nanorods showed an aspect ratio of 15, and the width was about 25 nm (EPAPS file).¹³ The polystyrene colloid was purchased from Duke Scientific with the size of 495 nm. The monolayered colloids and Au nanorod hybrid crystals were fabricated by the method of confined convective assembly.¹¹ We used an aqueous suspension of 495 nm polystyrene colloidal particles containing Au nanorods. The concentrations of colloidal particles and Au nanorods were 1.0 and 0.03–0.1 wt %, respectively. The above colloidal suspension was inserted into the gap approximately 50 μm of the front glass substrate (fixed substrate) and the back glass substrate (moving substrate) in a confined convective assembly setup (see Fig. 1). Subsequently, the back substrate was raised at a rate of 30 $\mu\text{m}/\text{s}$ while adding air flux toward the meniscus formed at the interface of the substrate and the colloidal suspension. The colloidal particles and Au nanorods then assembled into a monolayer on the back substrate. The

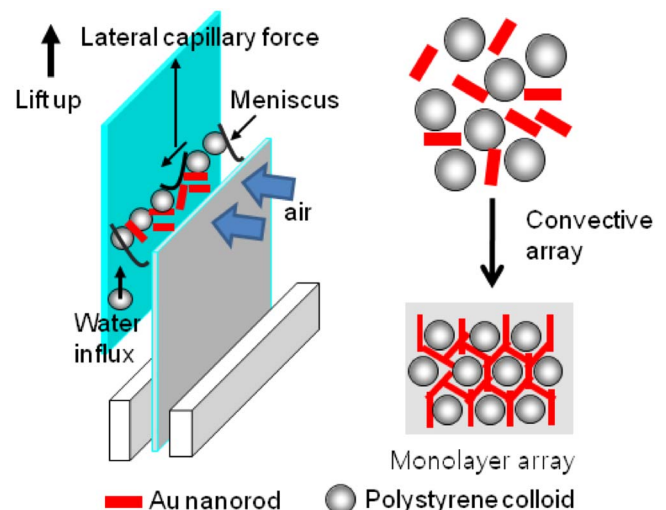


FIG. 1. (Color online) Schematic diagram of a low dimensional hybrid structure formed using a confined convective self-assembly method.

^{a)}Author to whom correspondence should be addressed. Electronic mail: upaik@hanyang.ac.kr.

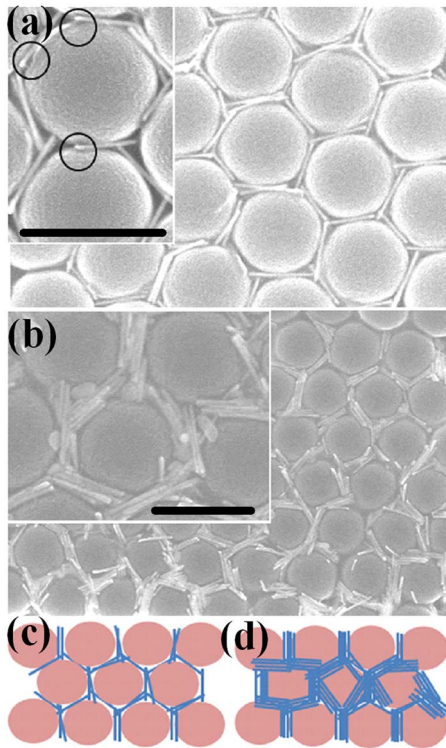


FIG. 2. (Color online) SEM micrograph of an array of Au nanorods formed along the hexagonally packed colloidal monolayer template for the cases of (a) 0.03 and (b) 0.09 wt %. Frames (c) and (d) provide corresponding schematic diagrams. Scale bar is 500 nm.

resulting binary combinations are similar to the ones fabricated using accelerated evaporation induced assembly methods.¹⁴ An advantage of the approaches described here is that they can be applied with small particles (<100 nm), and they enable fast (i.e., several minutes) fabrication times. Various nanomaterials with different geometries such as wires, rods, and spheres can be used.

Monolayer colloidal arrays can be achieved by adjusting the raising rate of the back substrate. At a rate of $45 \mu\text{m/s}$, the packing density in monolayers was low, and sparse morphologies were observed (EPAPS file).¹³ This behavior is due to insufficient time for colloids to move to the edge of the meniscus line. Au rods (0.03 wt %) were observed at both the locations of the colloidal layers and the vacancies. At a rate of $20 \mu\text{m/s}$, colloidal double layers formed with Au rod arrays between the colloids at both the bottom and upper layers (EPAPS file).¹³ Monolayer colloids and Au nanorod crystals formed smoothly at lift-up rates of $\sim 30 \mu\text{m/s}$. A hexagonal array of monolayered polystyrene colloids yielded organized collections of Au nanorods that were arrayed along the colloid circumferences (see Fig. 2). In this experiment, both spherical colloids and Au nanorods are under the convective forces that drive the colloids and the rods to move toward the meniscus line where a vigorous dispersion drying process occurs. The Au nanorods are also affected by microcapillarity between neighboring colloids. Colloid-colloid distances become narrower due to the lateral capillary forces as the water evaporates along the meniscus line (see Fig. 1). The Au nanorods become trapped within between the colloids and arrange themselves in arrayed layouts along the edges of the colloids.^{15–17}

The Au nanorod concentration in the colloid-rod dispersion was varied from 0.03 to 0.09 wt %. Figure 2(a) is for 0.03 wt % and Fig. 2(b) for 0.09 wt %. The results indicate that the density of Au nanorods in gaps between the colloids can be controlled. In particular, higher Au nanorod array densities are observed for 0.09 wt % [see Fig. 2(b)] than for 0.03 wt %. The colloid center-to-center distance was about 520 nm for both cases. In other words, no significant difference in Au rod concentration was observed for these two cases; the spaces for the Au nanorods between the colloids are similar. The rods extend higher in the spaces for the 0.09 wt % system, as is clear from the scanning electron microscopy (SEM) micrographs. The exposed colloid area at 0.09 wt % Au nanorod [Figs. 2(b) and 2(d)] is smaller than that of 0.03 wt % [Figs. 2(a) and 2(c)] by about 5%. In both cases, parallel arrays of Au nanorods with hexagonal symmetry are most prominent in the case of 0.03 wt %. When Au nanorod contents increased to 0.09 wt %, a failure of discrete six facets was observed. Organized parallel stacking of Au nanorods and platelike nanoparticles were also observed within the arrays [see the inset image of Fig. 2(b)]. We also note that the Au nanorods often tilt to form a slanting position, thereby frustrating the formation of an organized colloidal monolayer even at 0.03 wt % [see the inset of Fig. 2(a)].

This high density parallel stacking of Au nanorods can induce a functional surface plasmonic coupling and interference between the nearby Au rods when exposed to light. Although the optical properties of some Langmuir–Blgett–Schaefer assemblies of nanorods have been studied recently,^{18,19} the unusual structures presented here might lead to different effects of possible interest in optoelectronics. Transmittance spectra show that angle-dependent incomplete stop bands were achieved in polystyrene colloidal monolayers without the rods [see Fig. 3(a) inset]. As the incident angle increases from 0° to 30° , the peak position shifts toward higher wavelengths; corresponding iridescent colors can be observed by the eye. The magnitude of the stop band decreased at higher incident angle condition. The monolayered colloid/Au nanorod crystal (Au, 0.09 wt %) structure shows also angle-dependent incomplete stop bands. The peak was red shifted relative to the pure polystyrene colloidal monolayer crystal; the value of the shift was ~ 15 , 65, and 35 nm for 0° , 23° , and 30° incident angles, respectively [see Fig. 3(a)]. The magnitude decreased with increasing incident angle. The stop band is determined by a combination of the refractive index contrast in the periodic structure and the lattice constant. As mentioned previously, even with the Au rods, the colloid center-to-center distance remained ~ 520 nm, similar to the pure colloid case. We speculate, then, that the observed stop band shift is due mainly to the optical effects of the nanorods themselves. Redshifts in a photonic band gap are expected with increased effective refractive index for fixed lattice constant.^{20–22} Nanostructured Au nanomaterials have higher refractive index than that of bulk Au.^{23,24}

UV-visible absorbance (incident angle, 0°) spectra of the monolayered colloid/Au nanorod crystal shows a surface plasmonic resonance of a transverse mode centered at 525 nm [a dotted line in Fig. 3(b)] and an optical stop band at about 630 nm. The pure colloidal monolayer crystal showed no corresponding absorbance feature. The optical stop band due to the photonic crystal effects is clear at 615 nm. This

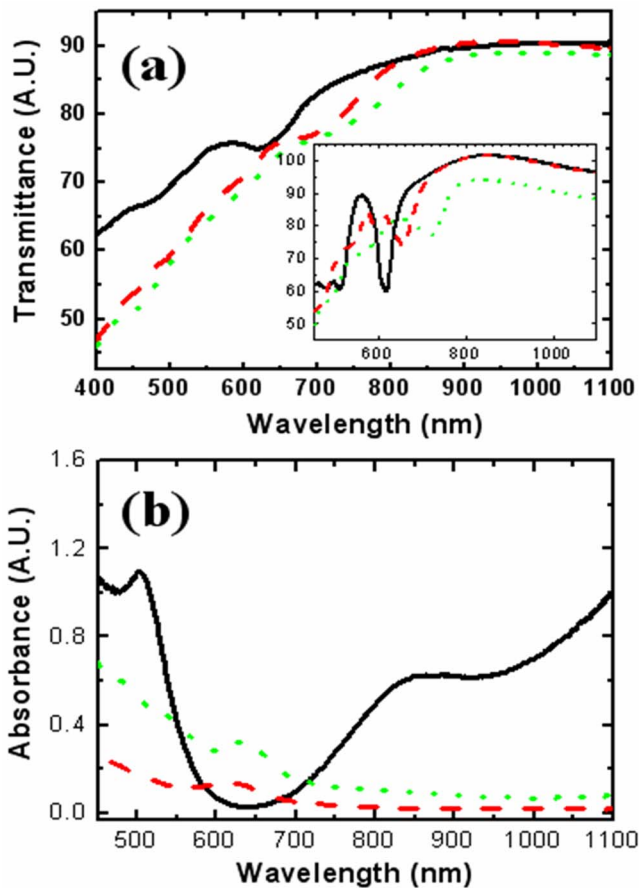


FIG. 3. (Color online) (a) Transmittance spectra of monolayer colloids and Au nanorod hybrid crystals. The black line corresponds to the case of 0° incident angle, red is for 23° , and green is for 30° . The inset shows transmittance spectra of a monolayer polystyrene colloids. (b) UV-visible absorbance spectra of Au nanorod aqueous dispersion (black), the monolayer colloid and Au nanorod hybrid crystal (green), and pure polystyrene colloidal monolayer (red).

peak is blueshifted compared to that of the monolayered colloid/Au nanorod crystal [see dashed line in Fig. 3(b)]. Although this structure does not show a deep photonic band gap valley in the UV-visible window, further development for more complete infiltration of Au rods in between the colloids could increase band gap effects. This proposed horizontal nanorod array protocol using spherical particles can be further studied to develop biosensors and optical materials, e.g., using arraying of semiconducting nanorods having controlled dimensions.

In summary, 2D structures of Au nanorods and colloids formed by convective assembly were demonstrated. The concentration of Au nanorods in the colloid-rod dispersion determined the array density in the colloid-nanorod hybrid crystals. The effects of the nanorods on the optical properties were examined. The stop band varied with incident light angle, as expected. Morphological control of low dimensional nanocomposites such as these might be important for various applications. In this context, systems analogous to those described here but with different material combinations, such as semiconductor rod-metal colloids, magnetic

tube-luminescent colloids, should be possible. Alternatively, related structures can offer interesting electrical properties. In a previous report,⁹ a transparent conductor based on CNT network, fabricated after colloid template discarding, was demonstrated. Likewise the Au rod-colloid system has potential to provide a transparent conductor after selective removal of the colloids. Here, recently reported methods for chemically bonding Au nanorods can be applied.²⁵

This work was supported by the Korea Foundation for International Cooperation of Science and Technology (KICOS) through a grant [Grant No. K2070400000307A050000310, Global Research Laboratory (GRL) Program] provided by the Korean Ministry of Education, Science and Technology (MEST) in 2008.

¹F. Caruso, *Top. Curr. Chem.* **227**, 145 (2003).

²Z. Tang, N. A. Kotov, and M. Giersig, *Science* **297**, 237 (2002).

³G. B. Sukhorukov, A. L. Rogach, B. Zebli, T. Liedl, A. G. Skirtach, K. Kehler, A. Antipov, N. Gaponik, A. S. Susha, M. Winterhalter, and W. J. Parak, *Small* **1**, 194 (2005).

⁴H. Y. Koo, D. K. Yi, S. J. Yoo, and D.-Y. Kim, *Adv. Mater. (Weinheim, Ger.)* **16**, 274 (2004).

⁵Y. Xia, B. Gates, Y. Yin, and Y. Lu, *Adv. Mater. (Weinheim, Ger.)* **12**, 693 (2000).

⁶J. C. Hulthen, D. A. Treichel, M. T. Smith, M. L. Duval, T. R. Jensen, and R. P. van Duyne, *J. Phys. Chem. B* **103**, 3854 (1999).

⁷K. Kempa, B. Kimball, J. Rybczynski, Z. P. Huang, P. F. Wu, D. Steeves, M. Sennett, M. Giersig, D. V. G. L. N. Rao, D. L. Carnahan, D. Z. Wang, J. Y. Lao, W. Z. Li, and Z. F. Ren, *Nano Lett.* **3**, 13 (2003).

⁸B. Fuhrmann, H. S. Leipner, and H.-R. Höche, *Nano Lett.* **5**, 2524 (2005).

⁹M. H. Kim, J. Y. Choi, H. K. Choi, S. M. Yoon, O. O. Park, D. K. Yi, S. J. Choi, and H. J. Shin, *Adv. Mater. (Weinheim, Ger.)* **20**, 457 (2008).

¹⁰N. D. Denkov, O. D. Velev, P. A. Kralchevsky, I. B. Yoshimura, H. Ivanov, and K. Nagayama, *Nature (London)* **361**, 26 (1993).

¹¹M. H. Kim, S. H. Im, and O. O. Park, *Adv. Funct. Mater.* **15**, 1329 (2005).

¹²T. K. Sau and C. J. Murphy, *Langmuir* **20**, 6414 (2004).

¹³See EPAPS Document No. E-APPLAB-94-001909 for A1. (a) TEM micrograph of Au nanorods (aspect ratio, ~ 15), for (b) SEM micrograph. A2. SEM micrographs of an Au rod-colloid structure formed at high lift-up rate ($45 \mu\text{m/s}$). The upper right shows that Au rods collect between the arrayed colloids. The lower right shows that Au rods appear in the vacancies. A3. SEM micrographs of the Au rod-colloid structure formed at a low lift-up rate ($20 \mu\text{m/s}$). The circles highlight regions where the colloids form a bilayer. The rods are arrayed in both the upper and the bottom layers. The inset provides an enlarged view of the upper layer. For more information on EPAPS, see <http://www.aip.org/pubservs/epaps.html>.

¹⁴V. Kitaev and G. A. Ozin, *Adv. Mater. (Weinheim, Ger.)* **15**, 75 (2003).

¹⁵D. K. Yi, M. J. Kim, and D.-Y. Kim, *Langmuir* **18**, 2019 (2002).

¹⁶G. Mason, *Br. Polym. J.* **5**, 101 (1973).

¹⁷D. K. Yi, E.-M. Seo, and D.-Y. Kim, *Appl. Phys. Lett.* **80**, 225 (2002).

¹⁸D. Zimmitsky, J. Xu, Z. Lin, and V. V. Tsukruk, *Nanotechnology* **19**, 215606 (2008).

¹⁹D. Whang, S. Jin, Y. Wu, and C. M. Lieber, *Nano Lett.* **3**, 1255 (2003).

²⁰S. H. Park and Y. Xia, *Langmuir* **15**, 266 (1999).

²¹Y. R. Lin, C. Y. Cuo, and S. Y. Lu, *Appl. Phys. A: Mater. Sci. Process.* **79**, 1741 (2004).

²²Z. Liang, A. S. Shusha, and F. Caruso, *Adv. Mater. (Weinheim, Ger.)* **14**, 1160 (2002).

²³K. Jain, X. Huang, I. H. El-Sayed, and M. A. El-Sayed, *Plasmonics* **2**, 107 (2007).

²⁴*Handbook of Chemistry and Physics*, edited by D. R. Lide (CRC, New York, 2008), Chap. 12–124.

²⁵K. K. Caswell, J. N. Wilson, U. H. F. Bunz, and C. J. Murphy, *J. Am. Chem. Soc.* **125**, 13914 (2003).